EVALUATION OF FAILURE CRITERIA FOR SHEAR STRENGTH IN WOOD ADHESIVE JOINTS WITH INCLINED GRAINS UNDER TENSION AND COMPRESSION LOADS

AVALIAÇÃO DE CRITÉRIOS DE FALHA PARA RESISTÊNCIA AO CISALHAMENTO EM JUNTAS ADESIVAS DE MADEIRA COM GRÃOS INCLINADOS SOB CARGAS DE TRAÇÃO E COMPRESSÃO

EVALUACIÓN DE LOS CRITERIOS DE FALLA DE LA RESISTENCIA AL CORTE EN UNIONES ADHESIVAS DE MADERA CON GRANOS INCLINADOS BAJO CARGAS DE TRACCIÓN Y COMPRESIÓN

Edgar Vladimiro Mantilla Carrasco[1] and Judy Norka Rodo Mantilla[2]

ABSTRACT
This study applied six failure criteria to estimate the shear strength of wood adhesive joints subjected to tension and compression loads as a function of fiber inclination. Shear stresses in the adhesive line were determined through experimental tests using specimens obtained from 12 Eucalyptus saligna beams. These specimens were prepared with variable fiber inclinations (0º, 15º, 30º, 45º, 60º, 75º, and 90º) relative to the load application, following the NBR 7190 standard. The experimental results were statistically analyzed in conjunction with the six failure criteria (Hankinson, DIN 1052, Tsai-Hill, Hyperbolic, Keylwerth, and Karlsen), allowing for the adaptation of the models to determine the shear strength of the adhesive line as a function of fiber inclination. In their original form, the Hankinson, DIN 1052, Tsai-Hill, and Hyperbolic models did not show statistical significance ($p < 0.05$). However, after modifications, all models demonstrated statistical significance, with the best fits being provided by the DIN 1052, Keylwerth, Hankinson, Karlsen, Hyperbolic, and Tsai-Hill models, in order of significance. Due to ease of application, the most recommended models for predicting the shear strength values of the adhesive line under compression and tension, as a function of fiber inclination, are the DIN 1052 and Hankinson formulas.

Keywords: Shear strength. Fiber inclination. Adhesive joints. Tension. Compression.

[1]Dr. in Structural Engineering
Federal University of Minas Gerais, School of Architecture, Belo Horizonte, MG, Brazil
E-mail: mantilla.carrasco@gmail.com
ORCID: 0000-0001-7870-0283
http://lattes.cnpq.br/3716965047168777
[2]Dr. in Civil Engineering
Federal University of Minas Gerais, School of Engineering, Belo Horizonte, MG, Brazil
E-mail: judynorka@gmail.com
ORCID: 0000-0001-7426-0970
http://lattes.cnpq.br/2270773118272768

RESUMO

Este estudo aplicou seis critérios de falha para estimar a resistência ao cisalhamento de juntas adesivas de madeira submetidas a cargas de tração e compressão em função da inclinação das fibras. As tensões de cisalhamento na linha adesiva foram determinadas por meio de ensaios experimentais utilizando corpos de prova obtidos de 12 vigas de Eucalyptus saligna. Esses corpos de prova foram preparados com inclinações variáveis das fibras (0º, 15º, 30º, 45º, 60º, 75º e 90º) em relação à carga aplicada, seguindo a norma NBR 7190. Os resultados experimentais foram analisados estatisticamente em conjunto com os seis critérios de falha (Hankinson, DIN 1052, Tsai-Hill, Hyperbolic, Keylwerth e Karlsen), permitindo a adaptação dos modelos para determinar a resistência ao cisalhamento da linha adesiva em função da inclinação da fibra. Em sua forma original, os modelos Hankinson, DIN 1052, Tsai-Hill e Hiperbólico não apresentaram significância estatística ($p < 0,05$). Entretanto, após modificações, todos os modelos demonstraram significância estatística, com os melhores ajustes sendo fornecidos pelos modelos DIN 1052, Keylwerth, Hankinson, Karlsen, Hiperbólico e Tsai-Hill, em ordem de significância. Devido à facilidade de aplicação, os modelos mais recomendados para previsão dos valores de resistência ao cisalhamento da linha adesiva sob compressão e tração, em função da inclinação das fibras, são as fórmulas DIN 1052 e Hankinson.

Palavras-chave: Resistência ao cisalhamento. Inclinação da fibra. Juntas adesivas. Tração. Compressão.

RESUMEN

En este estudio se aplicaron seis criterios de falla para estimar la resistencia al corte de las uniones adhesivas de madera sometidas a cargas de tracción y compresión en función de la inclinación de la fibra. Las tensiones de corte en la línea de adhesivo se determinaron mediante ensayos experimentales utilizando probetas obtenidas de 12 vigas de Eucalyptus saligna. Estas probetas fueron preparadas con inclinaciones de fibra variables (0º, 15º, 30º, 45º, 60º, 75º y 90º) en función de la carga aplicada, siguiendo la norma NBR 7190. Los resultados experimentales fueron analizados estadísticamente junto con los seis criterios de fallo (Hankinson, DIN 1052, Tsai-Hill, Hyperbolic, Keylwerth y Karlsen), permitiendo la adaptación de los modelos para determinar la resistencia al corte de la línea adhesiva en función de la inclinación de la fibra. En su forma original, los modelos Hankinson, DIN 1052, Tsai-Hill e Hiperbólico no mostraron significancia estadística ($p < 0,05$). Sin embargo, después de las modificaciones, todos los modelos demostraron significancia estadística, siendo los modelos DIN 1052, Keylwerth, Hankinson, Karlsen, Hyperbolic y Tsai-Hill los que proporcionaron los mejores ajustes, en orden de significancia. Por su facilidad de aplicación, los modelos más recomendados para predecir los valores de resistencia al corte de la línea adhesiva bajo compresión y tracción, en función de la inclinación de las fibras, son las fórmulas DIN 1052 y Hankinson.

Palabras clave: Resistencia al corte. Inclinación de fibra. Uniones adhesivas. Tracción. Compresión.

INTRODUCTION

Wood, a natural polymer primarily composed of cellulose, hemicellulose, and lignin, has been an essential construction material due to its mechanical properties and sustainability. Cellulose, the main structural component, provides wood with strength and rigidity, while hemicellulose and lignin offer cohesion and flexibility. The polymeric structure of wood, with its specifically oriented fibers, plays a crucial role in determining its mechanical properties, such as compressive and tensile strength [1].

The behavior of wood under compressive load, especially when applied at an angle to the fibers, has been extensively studied [2-7], with the influence varying according to the wood species. However, few studies address the influence of fiber inclination on shear strength in bonded joints under compression, and there is still controversy over which failure theories are most appropriate [8-12]. Conversely, the influence of fiber inclination on shear strength under tension is even less explored, with few studies available [13-21].

Adhesive polymers, such as epoxy, polyurethane, and phenol-formaldehyde resins, are widely used to form bonded joints between wood elements. These adhesives are chosen for their chemical adhesion properties, aging resistance, and ability to form durable bonds even under adverse conditions [22]. The shear strength of the adhesive line is a critical property that determines the effectiveness of bonded joints. This strength is influenced by several factors, including the chemical composition of the adhesive, the preparation of wood surfaces, the method of adhesive application, and curing conditions. The interaction between the adhesive and the wood is also significantly affected by the inclination of the wood fibers relative to the adhesive line [23].

Wood is a unique and variable material due to its natural defects and anisotropic characteristics. Thus, failure theories are quite complex [24-26]. There are no specific failure criteria to determine the shear strength of the adhesive line in compression as a function of wood fiber inclination. There are only failure criteria for wood compression, tension, and shear [24, 27, 28]. Among the numerous failure criteria, the Hankinson, Karlsen, DIN-1052, Keylwerth, Hyperbolic, and Tsai-Hill formulas are the most used to estimate the strength of wood when loaded at an angle to the fibers.

Researchers such as [3, 29-33] studied the influence of the direction of load application relative to wood fibers on shear strength, using principles and theories applied to wood compression strength. Some established theoretical models, generally considering orthotropic wood, while others established empirical models based on test results. The

types of failures that can occur in specimens, due to the anisotropy of the material, are difficult and complicated to evaluate due to the interaction of various mechanisms, such as material defects, load application conditions, environmental conditions, and wood mechanical properties in different directions [25].

The integrated analysis of studies on shear strength under compression and tension actions allows for a comprehensive understanding of the mechanical properties of bonded wood joints. Experimental tests were conducted with specimens obtained from 12 Eucalyptus saligna beams, made with varying fiber inclinations (0°, 15°, 30°, 45°, 60°, 75°, 90°) relative to the load application, following the [39] prescriptions. The test results were analyzed using six failure criteria: Hankinson, DIN 1052, Tsai-Hill, Hyperbolic, Keylwerth, and Karlsen.

Robust statistical analysis of the results allowed for the adaptation of models to determine the shear strength of the adhesive line as a function of wood fiber inclination. Initially, the Hankinson, DIN 1052, Tsai-Hill, and Hyperbolic models did not show statistical significance in their original format. However, with modifications made to the models, all formulations showed statistical significance, with the best fit, in order of significance: DIN 1052, Keylwerth, Hankinson, Karlsen, Hyperbolic, and Tsai-Hill.

The ease of application of the models was also considered, with the most suitable models for predicting the shear strength values of the adhesive line, both under compression and tension, as a function of fiber inclination being the DIN 1052 and Hankinson formulas. These models provide a solid basis for the development of more efficient bonded joints, significantly contributing to materials engineering and the construction of wooden structures.

Thus, wood, as a natural polymer, and the adhesive polymers used in bonded joints play crucial roles in determining the mechanical properties and structural performance of wooden constructions. Detailed investigation of the interactions between wood and adhesives, considering fiber orientation and load conditions, is essential for the development of accurate predictive models and the optimization of bonded joints in structural applications. This study provides a comprehensive and integrated understanding of the mechanical properties of bonded joints, providing valuable data for the design and construction of safer and more durable wooden structures.

METHOD

THEORETICAL ANALYSIS

The theoretical analysis of the shear test specimens (TSs) for the adhesive line under compression was conducted considering the classical theory of material strength. Figure 1a illustrates the test model for determining shear under compression, while Figure 1b shows the static equilibrium and Figure 1c presents the stress distribution. In Figure 2a, the TS for the adhesive line shear under tension is shown, consisting of two wooden plates covering the joint (bonded connection). The load transferred in this type of joint occurs through the shear stresses of the adhesive line. Due to the material discontinuity in the TSs, failure can occur by tension or compression perpendicular to the fibers. The simplified analysis considered the classical theory of materials, with the stress distribution along the adhesive line being nonlinear in the elastic phase and uniform in the plastic phase, as illustrated in Figure 2b.

Figure 1. (a) Test model for determining shear under compression, (b) Static equilibrium, and (c) Stress distribution.

a)   b)   c)
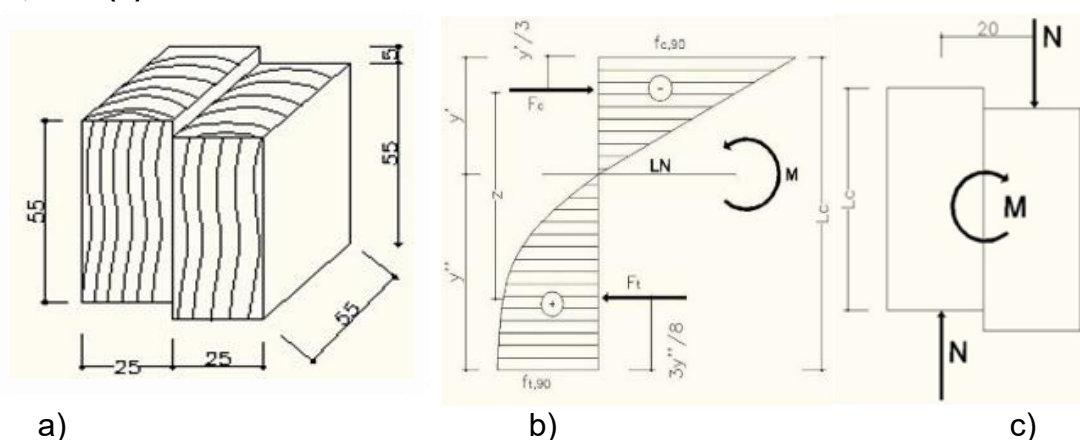
Source: The authors

Figure 2. (a) Test model for determining shear under tension, and (b) Static equilibrium.

a)   b)   c)
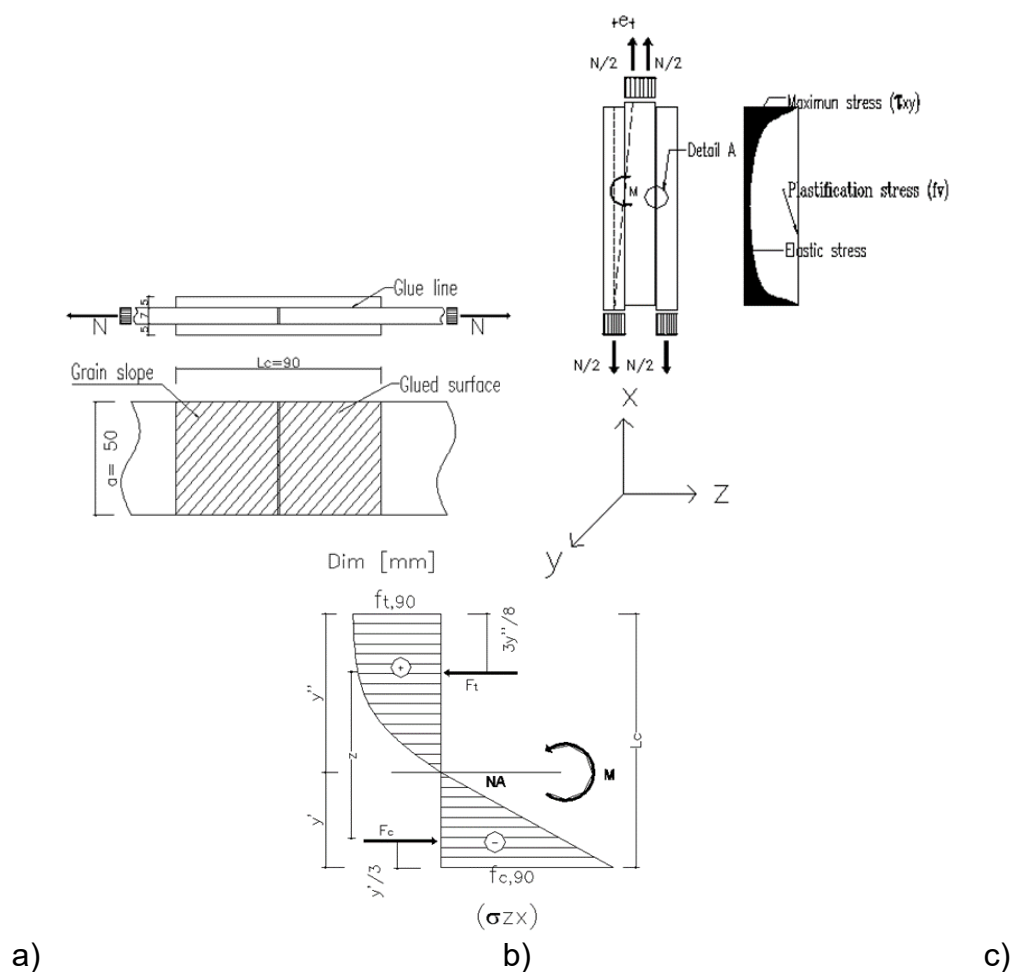
Source: The authors

To verify the failure mode, we considered the stress distribution through the adhesive line, which presents a triangular shape in the compressed zone and parabolic in the tensioned zone, as illustrated in Figures 1c and 2c. This distribution is due to the higher resistance of wood to compression perpendicular to the fibers compared to tension perpendicular to the fibers.

The theoretical analysis of the stress distribution was performed using the following equations:

Balancing forces, we have:

$$\sum F_h = 0 \quad \rightarrow \quad F_c = F_t \quad \rightarrow \quad \frac{f_{c,90} \cdot y' \cdot a}{2} = \frac{2 \cdot f_{t,90} \cdot y'' \cdot a}{3} \tag{1}$$

$$\sum M_{L.N.} = 0 \quad \rightarrow \quad M = F_c \left(y' - \frac{y'}{3} \right) + M = F_t \left(y'' - \frac{3 \cdot y''}{8} \right) \tag{2}$$

$$\text{the location of the NA is} \quad y' = \frac{L_c}{\left(\frac{3f_{c,90}}{4f_{t,90}} + 1 \right)} \quad \text{and} \quad y'' = \frac{L_c}{\left(\frac{4f_{t,90}}{3f_{c,90}} + 1 \right)} \quad ; z = \frac{2y'}{3} + \frac{5y''}{8} \tag{3}$$

$$L_c = y' + y'' \quad ; \quad M = N \cdot e \tag{4}$$

Where $f_{c,90}$ is the wood resistance to compressive stress perpendicular to grain, $f_{t,90}$ is the wood resistance to tensile stress perpendicular to grain, M is the bending moment, NA is the neutral axis, Lc is the length of the glue line, y' is the distance of the upper grain to the neutral axis, y'' is the distance of the lower grain to the neutral axis, a is the width of the piece, f_v is the wood resistance to shear stress, e is the eccentricity of the applied load, and A_c is the glued surface.

Therefore, the failure of the bonded joint occurs when the shear stress at all points of the adhesive line reaches the plasticization value of the shear stress of the adhesive or the adhesive-wood interface.

FAILURE THEORIES FOR WOOD

The six formulas presented below are derived from the application of various failure criteria used to obtain the compressive strength inclined to the fibers but can be used to predict the inclined fiber shear strength under tensile or compressive loading [20, 33]. According to [3], the empirical model proposed by Hankinson recommends using the exponent (n=2). [34] recommend an empirical model with an exponent (n=3) (Karlsen). The [35] DIN 1052 standard uses the equation with an exponent (n=1). Keylwerth [33] developed an empirical expression with an exponent (n=2) for the variation of the modulus of elasticity as a function of fiber inclination, which for strengths assumes a specific form. [28] and [24] present the Tsai-Hill theory as an extension of the Von Mises criterion for isotropic materials, while [36] proposes a hyperbolic formula with an exponent (n=0.01).

The following equations were modified to predict the shear strength of the adhesive line under compression and tension inclined to the wood fibers:

$$f_{va?,\theta} = \frac{f_{va?,0} \times f_{va?,90}}{f_{va?,0} \times \sin(\theta)^n + f_{va?,90} \times \cos(\theta)^n} \tag{5}$$

$$f_{va?,\theta} = \frac{f_{va?,0}}{1 + \left(\frac{f_{va?,0}}{f_{va?,90}} + 1\right) \times \sin(\theta)^n} \tag{6}$$

$$f_{va?,\theta} = f_{va?,0} - \left(f_{va?,0} - f_{va?,90}\right) \times \sin(\theta)^n \tag{7}$$

$$f_{va?,\theta} = \frac{f_{v,0}}{\left(\cos(\theta)^n - \frac{f_{va?,0}}{f_{va?,90}} \times \sin(\theta)^n\right) \times \cos(2\theta) + \frac{f_{va?,0}}{f_{va?,45}} \times \sin(2\theta)^n} \tag{8}$$

$$\frac{1}{f_{va?,\theta}^2} = \frac{\cos(\theta)^{2n}}{f_{va?,0}^2} - \frac{\cos(\theta)^n \sin(\theta)^n}{f_{va?,0}^2} + \frac{\sin(\theta)^{2n}}{f_{va?,90}^2} \tag{9}$$

$$f_{va?,\theta} = \frac{f_{vac,0} \times f_{vac,90}}{f_{va?,0} \sinh(n\theta) + f_{va?,90} \cosh(n\theta)} \quad \text{ou}$$

$$f_{vac,\theta} = \frac{2f_{vac,0} \times f_{vac,90}}{e^{n\theta}(f_{va?,0} + f_{va?,90}) + e^{-n\theta}(f_{va?,90} - f_{va?,0})} \tag{10}$$

Where: $f_{va?,\square}$ = shear strength inclined to the fibers under compression or tension, $f_{va?,\square}$ = shear strength parallel to the fibers under compression or tension, $f_{va?,\square\square}$ = shear strength normal to the fibers under compression or tension, $f_{va?,\square\square}$ = shear strength at 45 degrees to the fibers when subjected to compression or tension, and θ = angle between the fibers and the load application.

There is controversy among authors about the value of the exponent (n) of the trigonometric terms in equations 4 to 8. Some authors indicate different coefficients depending on the type of loading, while others indicate different coefficients for different moisture contents of the wood.

MATERIALS

To ensure a representative sampling, the wood beams were randomly selected in small batches from sawmills at different times. The wood used for the TSs was Eucalyptus saligna (*E. saligna Sm., Myrtaceae*), with a maximum thickness of 55 mm and varying widths. The wood moisture content ranged from 11.44% to 25.33%, while the apparent density varied between 690 kg/m³ and 860 kg/m³. This variation is relevant to ensure that the test results are widely applicable to different moisture and density conditions found in practice.

The choice of adhesives was based on the principle that wood, being highly polar, presents good affinity with adhesives of similar or intermediate polarity. According to [22, 37, 38], the most suitable adhesives for structural applications include polyvinyl acetate, phenol-formaldehyde, resorcinol-formaldehyde, urea-formaldehyde, melamine, and melamine-urea-formaldehyde. For the tests, a resorcinol-based adhesive was chosen. This adhesive consists of a liquid resin used with a powder catalyst, with proportions recommended by the manufacturer (Hexion Chemical Industry and Trade). Both the resin and the catalyst were weighed on an electronic balance with centigram precision and then mixed until complete homogenization. The temperature during preparation and application ranged from 20°C to 30°C.

The TSs were made from twelve randomly chosen beams, whose surfaces were carefully prepared. The adhesive was applied by brushing, followed by the application of 1.5 MPa pressure, as recommended by the manufacturer. This pressure was maintained for a minimum period of eight hours to ensure proper curing of the adhesive.

TEST SPECIMENS (TSS)

To evaluate the shear strength of the adhesive line under compression

96 TSs were made, with 84 TSs for adhesive line shear tests, with one of the TS elements bonded with fibers inclined relative to the load application (12 TSs for each inclination) and 12 TSs for moisture and density (following the recommendations of [39] and [40]), Figure 3.

**Figure 3. Test specimens with variable fiber inclination relative to the applied load.**
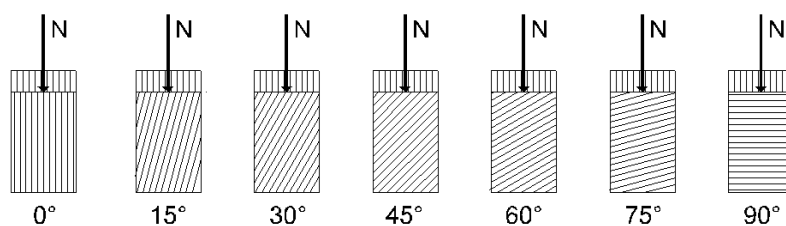
Source: The authors

To evaluate the shear strength of the adhesive line under tension

The TSs were designed according to the tensile TSs proposed by [41] and the Brazilian standard [39]. The side plates of the TSs were prepared by varying the inclination of the wood fibers relative to the applied load (Figure 4). A total of 96 TSs were made, with 84 TSs for adhesive line shear strength tests, with the side wood plates bonded with fibers at an angle relative to the load application (12 TSs per angle) and 12 TSs for moisture and density (following the recommendations of [39] and [40]), Figure 4.

Figure 4. Test specimens with varied grain angles in relation to the load applied (mm).
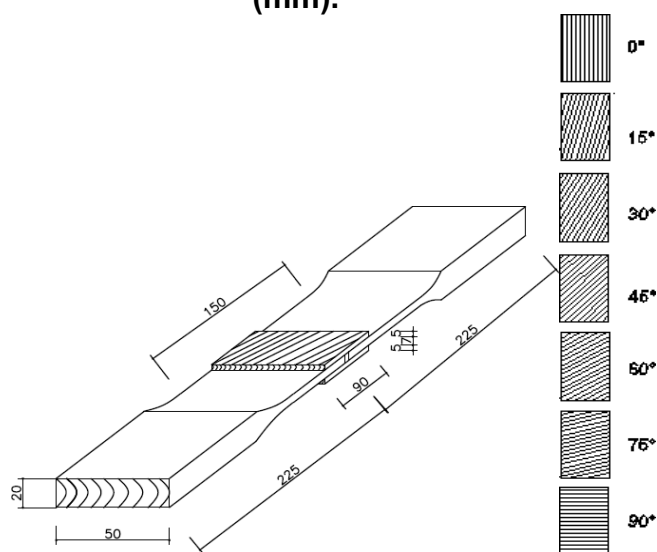
Source: The authors

For wood characterization

The dimensions of the TSs for shear tests were: 6.4 cm x 5 cm x 5 cm, with a small step of 1.4 cm x 2 cm x 5 cm for fixing the test equipment, and a bonded area of 5 cm x 5 cm. To determine moisture and density, the dimensions were: 2 cm x 3 cm x 5 cm [39, 40].

EXPERIMENTAL PROCEDURE

The shear tests of the adhesive line, both under compression and tension, were performed on an Instron/Emic universal testing machine with a capacity of 300 kN. The applied load was monotonic at a rate of 2.5 MPa per minute until the TSs failed. An abrupt and instantaneous failure of the test specimens was observed, characterizing a brittle failure. After each shear test, moisture and density tests were performed to obtain values at the time of the test, allowing the correction of the result to the reference moisture content of 12%. For this, equation 11 was used [39].

$$f_{va?,\theta,12} = f_{va?,\theta,U\%} \left(1 + \frac{2 \times (U\% - 12)}{100}\right) \qquad (11)$$

Where: $f_{va?,\square,12}$ = shear strength of the adhesive line under compression or tension inclined at an angle (θ) relative to the wood fibers, at the reference moisture content of 12%; $f_{va?,\square,U\%}$ = shear strength of the adhesive line under compression or tension inclined at an angle (θ) relative to the wood fibers, at the moisture content U%, at the time of the test.

For the statistical analysis of the test results, we used the Minitab 16 program, especially for null hypothesis tests and one-way ANOVA.

RESULTS AND DISCUSSION

The results presented here are crucial for understanding how wood and polymeric adhesives interact under different loading conditions and how these interactions affect structural integrity.

Table 1 presents the shear stress results at adhesive failure under compression, tension, and in the wood, corrected for the reference moisture content of 12%. The stresses vary with the inclination of the wood fibers, demonstrating the significant influence of fiber orientation on shear strength.

Figure 5 shows the graph of adhesive shear stress under compression versus fiber inclination, displaying the experimental values (including the confidence interval) and the six
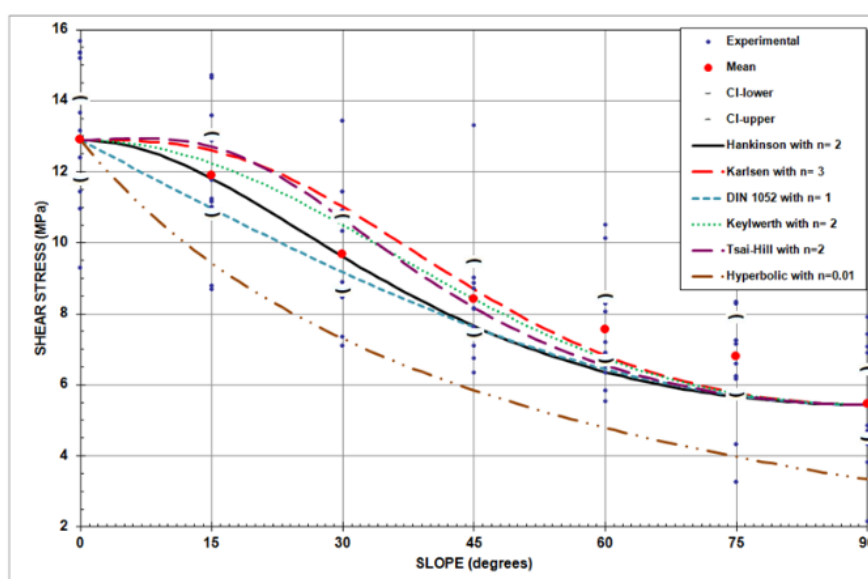
equations with the exponent suggested by the authors. It is noted that the curves of all equations fall outside the confidence interval of the experimental results for at least one fiber inclination, indicating that the "n" exponents of the equations should differ from those suggested by the authors.

Table 1: Shear stress of the adhesive line under compression, tension, and shear stress of the wood, corrected for standard moisture of 12% (MPa).

B	Ty	0°	15°	30°	45°	60°	75°	90°	B	Ty	0°	15°	30°	45°	60°	75°	90°
1	C	11.43	11.02	10.91	8.13	6.90	4.32	3.81	7	C	10.95	8.79	7.10	6.74	5.54	5.66	4.69
	T	10.19	9.27	8.96	3.09	2.99	1.96	1.75		T	13.84	11.68	11.92	5.06	2.65	1.56	1.08
	W	15.65	12.87	12.25	13.28	10.09	9.06	8.44		W	12.64	12.04	10.95	9.63	8.43	7.34	6.50
2	C	14.15	11.76	10.86	9.47	8.27	8.27	7.07	8	C	13.16	13.13	11.45	8.16	10.13	7.89	7.89
	T	7.97	7.07	7.37	1.59	1.00	0.80	0.40		T	13.29	11.84	11.84	3.82	2.24	1.45	1.18
	W	17.14	15.44	14.35	11.36	12.95	10.16	9.76		W	14.47	11.97	10.00	9.60	9.74	6.71	6.97
3	C	9.29	8.68	7.35	6.33	5.82	3.27	2.14	9	C	13.66	12.88	9.75	8.71	8.06	7.15	6.50
	T	9.60	9.60	8.68	5.92	3.27	2.25	0.82		T	12.62	12.49	10.01	7.67	4.03	1.17	1.04
	W	18.68	16.95	14.19	11.84	11.64	11.74	12.56		W	15.87	15.35	13.40	15.35	9.23	10.93	9.49
4	C	15.34	14.65	10.32	8.85	6.88	6.59	4.33	10	C	15.68	13.58	13.44	13.30	10.50	10.50	7.42
	T	12.00	10.03	7.57	5.80	2.85	1.87	1.28		T	14.42	13.72	13.16	7.70	4.48	1.82	0.84
	W	17.85	16.12	14.75	12.68	13.08	13.47	11.31		W	17.78	16.10	12.32	13.44	11.90	11.06	11.48
5	C	15.35	14.71	8.47	7.09	7.20	7.24	6.88	11	C	11.72	11.23	8.88	7.63	6.34	6.24	4.90
	T	11.11	10.16	9.21	6.56	3.60	2.75	1.91		T	10.26	9.31	8.51	4.78	2.66	1.56	1.01
	W	14.29	9.53	9.84	12.28	11.43	7.94	7.94		W	15.19	12.98	11.97	11.08	9.76	8.85	8.30
6	C	12.39	11.15	8.56	9.01	8.56	8.33	4.84	12	C	11.62	11.16	8.80	7.51	6.52	6.15	4.81
	T	11.60	10.02	8.22	6.76	2.93	1.46	0.45		T	10.18	9.23	8.42	4.68	2.61	1.50	0.90
	W	14.08	14.19	11.60	10.47	10.14	9.01	8.22		W	14.05	12.14	11.33	10.83	9.72	8.78	8.22
M	C	12,90	11,90	9,66	8,41	7,56	6,80	5,44	SD	C	2,00	1,98	1,83	1,81	1,59	1,92	1,71
	T	11,42	10,37	9,49	5,29	2,94	1,68	1,06		T	1,90	1,78	1,86	1,84	0,89	0,50	0,45
	W	15,64	13,81	12,25	11,82	10,68	9,59	9,10		W	1,87	2,23	1,64	1,69	1,49	1,95	1,87

B = Beam, Ty = Type, C = Compression, T = Tension, W = Wood, M = Mean, SD = Standard Desviation.

Figure 5. Shear stress of the adhesive line under compression relative to fiber inclination.

Source: The authors

Figure 6 presents the graph of shear stress of the adhesive line under tension relative to fiber inclination, showing the experimental values (including the confidence interval) and the six equations with the exponent suggested by the authors.

Figure 6. presents the graph of shear stress of the adhesive line under tension relative to fiber inclination, showing the experimental values (including the confidence interval) and the six equations with the exponent suggested by the authors.
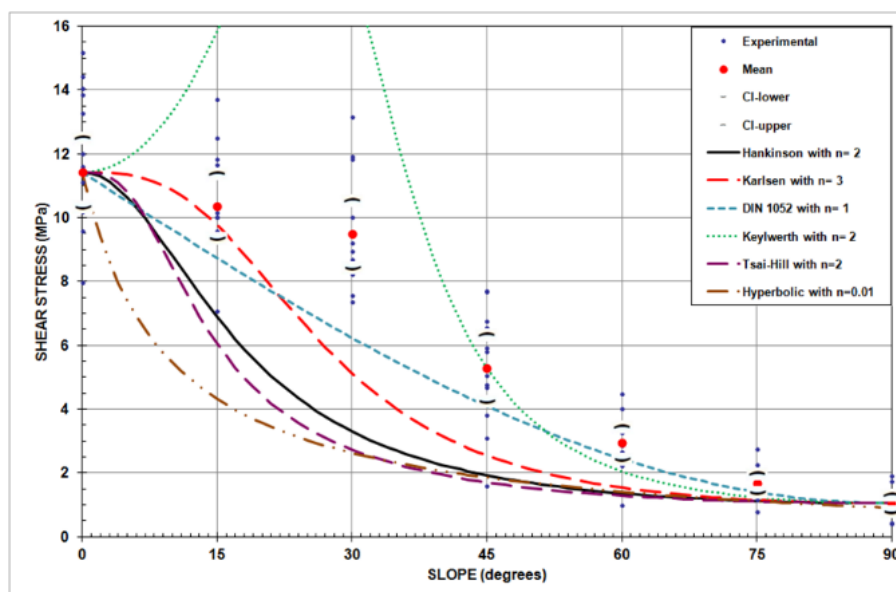
Source: The authors

Assuming the experimental results follow a normal distribution, as shown by the Anderson-Darling test (p-value > 0.05) for both tension and compression, and through the statistical analysis of the null difference hypothesis, for comparing pairs of individuals and groups of individuals, the experimental values were compared with the equivalents calculated by equations 8 to 13, using the variation of the exponents (n) of the trigonometric functions. Thus, the value of the exponent n that provides the best fit for each equation was obtained. Table 2 presents the results of the null difference tests, obtained with the application of the Minitab 16 program and its analysis.

Observing Table 2, it is noted: the Hankinson expression (equation 5) has statistical validity for shear under compression, provided the exponent "n" is in the range $2.19 \leq n \leq 2.63$, and the exponent that provides the best fit is n = 2.386. For shear under tension, the range is $3.97 \leq n \leq 4.79$, and the exponent that allows the best fit is n = 4.364. The traditionally used value of n = 2 does not have statistical validity and shows high rejection. The values found by [31,12] for Perobamica wood (*Aspidosperma populifolium*), when

analyzing the influence of wood fiber direction on shear strength, also lack statistical validity (n = 2.05 and range of 1.88 ≤ n ≤ 2.05).

Table 2: Results of tests of zero difference between the experimental values and equations 8 to 13, varying the exponent "n" (significance level of 95%), with t_{cr} = 1.992.

Eq.	Shear stress	n	Mean Difference	t	p	Confidence interval
5	C	2.386	0.000	0.00	0.999	-0.737 ; 0.002
	T	4.346	0.000	0.00	1.000	-0.402 ; 0.402
6	C	3.113	0.000	0.00	1.000	-0.310 ; 0.310
	T	6.485	0.000	0.00	0.999	-0.284 ; 0.284
7	C	1.791	0.000	0.00	0.999	-0.275 ; 0.275
	T	1.887	-0.000	0.00	0.999	-0.249 ; 0.249
8	C	2.409	0.000	0.00	0.999	-0.246 ; 0.246
	T	3.60	-0.262	-1.16	0.250	-0.712 ; 0.188
9	C	1.528	0.000	0.00	0.999	-0.348 ; 0.348
	T	3.722	0.001	0.00	0.996	-0.454 ; 0.456
10	C	0.0043	0.000	0.00	0.998	-0.264 ; 0.264
	T	0.0018	0.000	0.00	0.999	-0.485 ; 0.484

Eq. 5 = Hankinson, 6 = Karlsen, 7 = DIN-1052, 8 = Keylwerth, 9 = Tsai-Hill, 10 = Hyperbolic. C = Compression, T = Tension.

For the Karlsen expression (equation 6) to have statistical validity for shear under compression, the exponent "n" must be in the range of 2.50 ≤ n ≤ 4.07, and the exponent that provides the best fit is n = 3.113. For shear under tension, the range is 5.60 ≤ n ≤ 7.63, and the exponent that provides the best fit is n = 6.485. The traditionally used value, recommended by [34], of n = 3 has statistical validity. However, the value found by [31] is different, n = 2.13, lacks statistical validity, and shows high rejection.

The DIN-1052 expression (equation 7) will have statistical validity for shear under compression, provided the exponent "n" is in the range of 1.45 ≤ n ≤ 2.29, and the exponent that allows the best fit is n = 1.791. For shear under tension, the range is 1.64 ≤ n ≤ 2.19, and the exponent that provides the best fit is n = 1.887. The value used by this standard, n = 1, is outside the range, indicating it lacks statistical validity. The value found by [31], n = 1.21, lacks statistical validity and shows high rejection.

For the Keylwerth expression (equation 8), it was not possible to find the lower limit of the statistical validity range for the expression's exponent, both for shear under compression and tension. It seems there is a singularity in the expression that allows finding another exponent value that provides a highly significant model fit. The range for shear under compression is "open value" ≤ n ≤ 2.93, and the exponent that provides the

best fit is n = 2.409. For shear under tension, the range is "open value" ≤ n ≤ 4.79, and the exponent that provides the best fit is n = 3.60. The traditionally used value, n = 2, recommended by [3], has statistical validity. The value found by [31] is different, n = 2.04, with statistical validity.

Still analyzing Table 2, it is observed that the expression provided by the Tsai-Hill theory (equation 9) has statistical validity for shear under compression, provided the exponent "n" is in the range 1.34 ≤ n ≤ 1.78, and the exponent that provides the best fit is n = 1.528. For shear under tension, the range is 3.31 ≤ n ≤ 4.205, and the exponent that provides the best fit is n = 3.722. The value indicated by [24, 25], of n = 2, lacks statistical validity and shows high rejection.

The Hyperbolic formula (equation 10) has statistical validity for shear under compression, provided the exponent "n" is in the range $38.7 \times 10^{-4} \leq n \leq 47.9 \times 10^{-4}$, and the exponent that provides the best fit is $n = 43.34 \times 10^{-4}$. For shear under tension, the range is $17.4 \times 10^{-4} \leq n \leq 28.3 \times 10^{-4}$, and the exponent that provides the best fit is $n = 22.24 \times 10^{-4}$. The value indicated by [24, 25], of $n = 100 \times 10^{-4}$, lacks statistical validity and shows high rejection.

For a more robust evaluation in choosing the best model representing the experimental results, a One-way ANOVA analysis was conducted. In this context, the methods of Dunnett, Tukey, and Fisher were used. All theoretical equations have high significance.

Finally, to visualize the variation of shear stresses as a function of fiber inclination, from all equations, within the confidence interval of the experimental adhesive line shear stresses under compression and tension (significance level of 95%), a graphical representation of the shear stresses of these equations was prepared, using the exponent "n" that resulted in the greatest statistical significance, and the experimental values, Figures 7 and 8.

Figure 7. Shear stress of the adhesive line under compression relative to fiber inclination. equations with the "n" exponent that showed the greatest statistical significance.
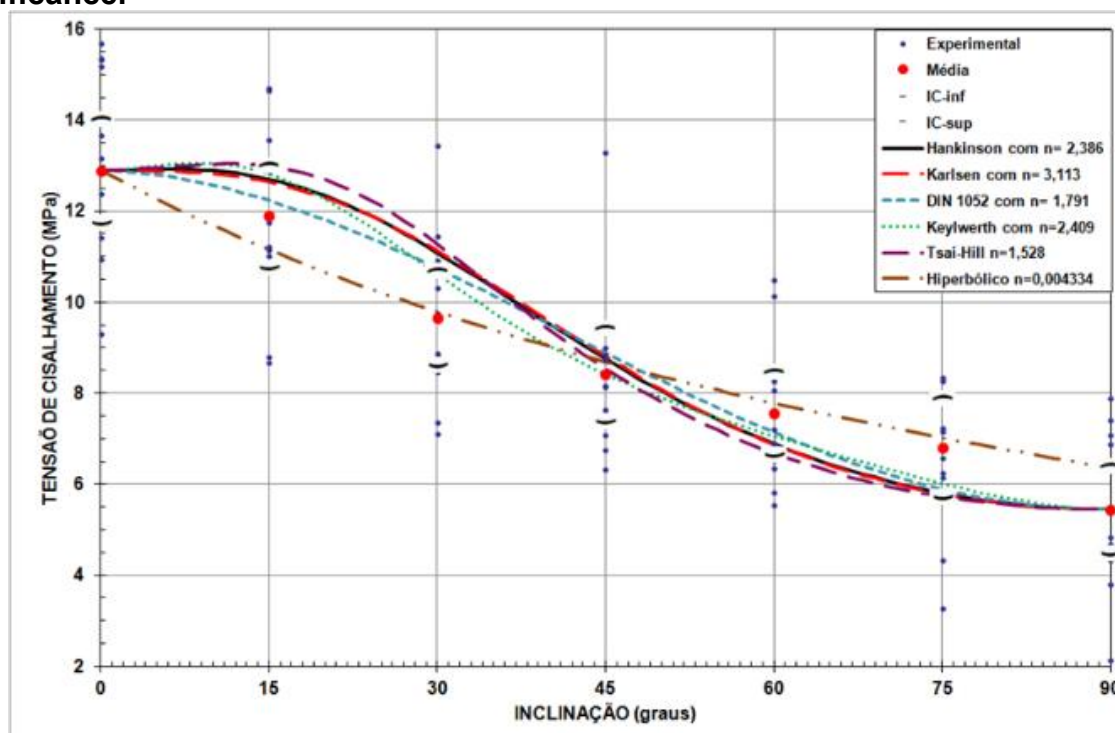
Source: The authors

Figure 8. Shear stress of the adhesive line under tension relative to fiber inclination. equations with the "n" exponent that showed the greatest statistical significance.
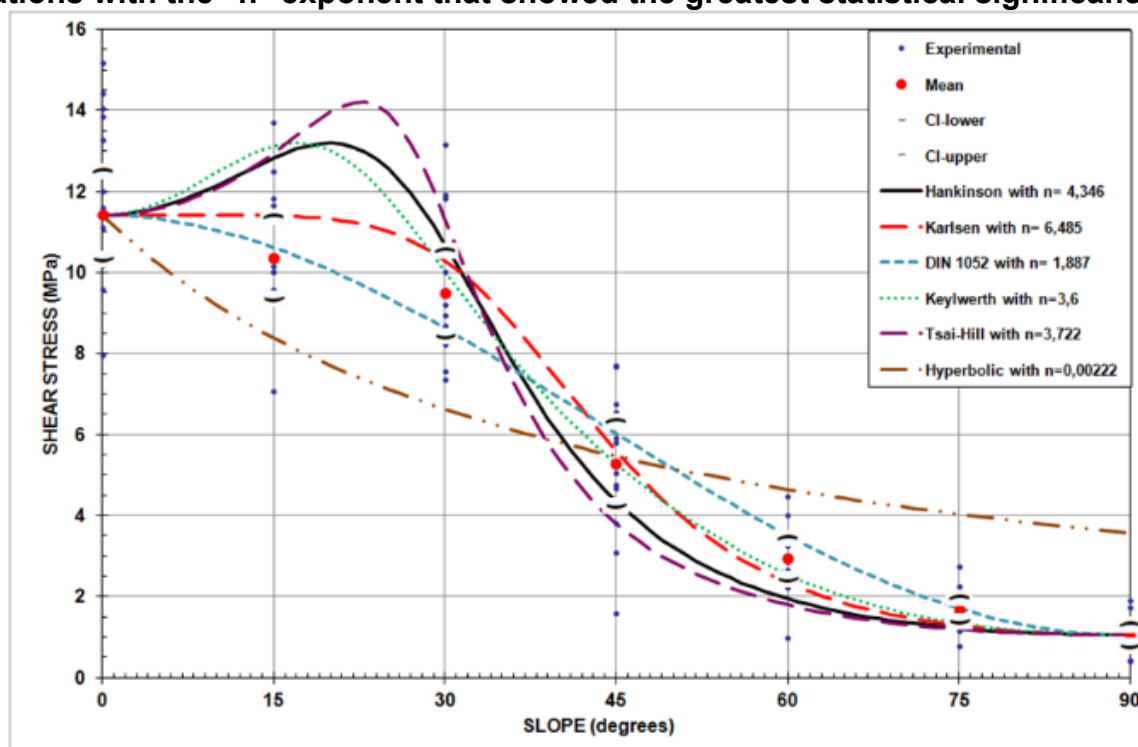
Source: The authors

From the analysis of the graphs in Figure 7 (shear under compression) and considering the statistical analyses, it can be stated that, in order of significance, the equations that best represent the experimental values of shear stress under compression are: DIN 1052 (equation 12), Keylwerth (equation 13), Hankinson (equation 14), Karlsen (equation 15), Hyperbolic (equation 16), and Tsai-Hill (equation 17).

$$f_{vac,\theta} = f_{vac,0} - \left(f_{vac,0} - f_{vac,90}\right) \times \sin(\theta)^{2,386} \qquad (12)$$

$$f_{vac,\theta} = \frac{f_{v,0}}{\left(\cos(\theta)^{2,409} - \frac{f_{vac,0}}{f_{vac,90}} \times \sin(\theta)^{2,409}\right) \times \cos(2\theta) + \frac{f_{vac,0}}{f_{vac,45}} \times \sin(2\theta)^{2,409}} \qquad (13)$$

$$f_{vac,\theta} = \frac{f_{vac,0} \times f_{vac,90}}{f_{vac,0} \times \sin(\theta)^{2,386} + f_{vac,90} \times \cos(\theta)^{2,386}} \qquad (14)$$

$$f_{vac,\theta} = \frac{f_{vac,0}}{1 + \left(\frac{f_{vac,0}}{f_{vac,90}} + 1\right) \times \sin(\theta)^{3,113}} \qquad (15)$$

$$f_{vac,\theta} = \frac{f_{vac,0} \times f_{vac,90}}{f_{vac,0} \sinh(0,004334\theta) + f_{vac,90} \cosh(0,004334\theta)} \quad ou$$
$$f_{vac,\theta} = \frac{2 f_{vac,0} \times f_{vac,90}}{e^{0,004334\theta}\left(f_{vac,0} + f_{vac,90}\right) + e^{-0,004334\theta}\left(f_{vac,90} - f_{vac,0}\right)} \qquad (16)$$

$$\frac{1}{f_{vac,\theta}^2} = \frac{\cos(\theta)^{3,056}}{f_{vac,0}^2} - \frac{\cos(\theta)^{1,528} \sin(\theta)^{1,528}}{f_{vac,0}^2} + \frac{\sin(\theta)^{3,056}}{f_{vac,90}^2} \qquad (17)$$

Analyzing the graphs in Figure 8 (shear under tension) and considering the statistical analyses, it can be stated that, in order of significance, the equations that best represent the experimental values of shear stress under tension are: DIN 1052 (equation 18) and Karlsen (equation 19).

$$f_{vat,\theta} = f_{vat,0} - \left(f_{vat,0} - f_{vat,90}\right) \times \sin(\theta)^{1,887} \qquad (18)$$

$$f_{vat,\theta} = \frac{f_{vat,0}}{1 + \left(\frac{f_{vat,0}}{f_{vat,90}} + 1\right) \times \sin(\theta)^{6,485}} \qquad (19)$$

The results obtained demonstrate that the shear resistance of the adhesive line is significantly influenced by the inclination of the wood fibers. The equations adjusted with the new "n" exponents provide a better fit to the experimental data, indicating that the traditionally used values are not suitable for all situations. Compression and tension tests allow for a more comprehensive understanding of the mechanical behavior of structural woods and the adhesives used. Robust statistical analysis, including the use of ANOVA models, confirms the significance of the adjusted equations.

CONCLUSIONS

Regarding failure criteria models, none of the six mathematical models evaluated (Hankinson, DIN 1052, Tsai-Hill, Hyperbolic, Keylwerth, and Karlsen) showed statistical significance in their original form. This indicates that the traditional exponents used in these models are not adequate for accurately predicting the shear resistance of the adhesive line as a function of fiber inclination.

With the modifications made to the models, all equations showed statistical significance. The adjustments to the "n" exponents resulted in models that better fit the experimental data, providing more accurate predictions of shear resistance. The models that showed the best fit, in order of significance, were: DIN 1052, Keylwerth, Hankinson, Karlsen, Hyperbolic, and Tsai-Hill.

Due to ease of application and accuracy in predictions, the most recommended models for estimating the shear resistance values of the adhesive line, both in compression and tension, as a function of fiber inclination, are: DIN 1052, Hankinson, and Keylwerth.

The analysis of shear tests in compression and tension provides a more complete understanding of the mechanical behavior of structural woods and polymeric adhesives. These results are crucial for the development of more accurate and reliable models, which can be used in the design and construction of wooden structures.

The resorcinol-based adhesive proved effective in bonding wood pieces, showing shear resistance consistent with theoretical predictions. The application of DIN 1052 and Karlsen models, after adjustments to the exponents, provided the best estimates for the shear resistance values of the adhesive line under tension and compression.

REFERENCES

1. Antonio, S. L. (2025). Technological innovations and geomechanical challenges in Midland Basin drilling. *Brazilian Journal of Development, 11*(3), e78097. https://doi.org/10.34117/bjdv11n3-005

2. ASTM. (2007). *Standard methods of testing small clear specimens of timber* (ASTM D-143-94). ASTM International.

3. Blyberg, L., Serrano, E., Enquist, B., & Sterley, M. (2012). Adhesive joints for structural timber/glass applications: Experimental testing and evaluation methods. *International Journal of Adhesion & Adhesives, 35*, 76–87. https://doi.org/10.1016/j.ijadhadh.2012.02.008

4. Bodig, J., & Jayne, B. A. (1993). *Mechanics of wood and wood composites* (2nd ed.). Krieger Publishing.

5. Budhe, S., Banea, M. D., de Barros, S., & da Silva, L. F. M. (2017). An updated review of adhesively bonded joints in composite materials. *International Journal of Adhesion & Adhesives, 72*, 30–42. https://doi.org/10.1016/j.ijadhadh.2016.10.010

6. Burdurlu, E., Kiliç, G., Elibol, C., & Kiliç, M. (2006). The shear strength of Calabrian pine (*Pinus brutia* Ten.) bonded with polyurethane and polyvinyl acetate adhesives. *Journal of Applied Polymer Science, 99*(6), 3050–3061. https://doi.org/10.1002/app.22905

7. Carrasco, E. V. M. (1984). *Ligações estruturais de madeira por adesivos* [Master's thesis, São Paulo University].

8. Carrasco, E. V. M., & Mantilla, J. N. R. (2013). Applying failure criteria to shear strength evaluation of bonded joints according to grain slope under compressive load. *International Journal of Engineering & Technology, 13*(4), 19–25.

9. Carrasco, E. V. M., & Mantilla, J. N. R. (2015). Failure criteria for shear strength evaluation of bonded joints according to grain slope under tension load. *BioResources, 10*(2), 1845–1855. https://doi.org/10.15376/biores.10.2.3602-3614

10. Carrasco, E. V. M., & Mantilla, J. N. R. (2016). Influência da inclinação das fibras da madeira na sua resistência ao cisalhamento. *Ciência Florestal, 26*(2), 535–543. https://doi.org/10.5902/1980509822754

11. Chazzaoui, T. A. M. (2025). The impact of Brexit on international logistics: Challenges and opportunities for businesses. *Brazilian Journal of Development, 11*(5), e79899. https://doi.org/10.34117/bjdv11n5-066

12. Chen, X. D., Cheng, Y. Y., Chan, A. N., Holloway, D., & Nolan, G. (2022). Anisotropic tensile characterisation of *Eucalyptus nitens* timber above its fibre saturation point, and its application. *Polymers, 14*(12), 2390. https://doi.org/10.3390/polym14122390

13. Delci, C. A. M. (2025). The effectiveness of Last Planner System (LPS) in infrastructure project management. *Revista Sistemática, 15*(2), 133–139. https://doi.org/10.56238/rcsv15n2-009

14. Deutsches Institut für Normung. (2008). *Design of timber structures - General rules and rules for buildings* (DIN 1052). DIN.

15. Dinwoodie, J. M. (1975). Timber: A review of the structure-mechanical property relationship. *Journal of Microscopy, 104*(1), 3–32. https://doi.org/10.1111/j.1365-2818.1975.tb04002.x

16. Filho, W. L. R. (2025a). The role of AI in enhancing identity and access management systems. *International Seven Journal of Multidisciplinary, 1*(2). https://doi.org/10.56238/isevmjv1n2-011

17. Filho, W. L. R. (2025b). The role of Zero Trust Architecture in modern cybersecurity: Integration with IAM and emerging technologies. *Brazilian Journal of Development, 11*(1), e76836. https://doi.org/10.34117/bjdv11n1-060

18. Follrich, J., Teischinger, A., Gindi, W., & Müller, U. (2007). Effect of grain angle on shear strength of glued end grain to flat grain joints of defect-free softwood timber. *Wood Science and Technology, 41*(6), 501–509. https://doi.org/10.1007/s00226-007-0136-7

19. Follrich, J., Vay, O., Veigel, S., & Müller, U. (2010). Bond strength of end-grain joints and its dependence on surface roughness and adhesive spread. *Journal of Wood Science, 56*(5), 429–434. https://doi.org/10.1007/s10086-010-1118-1

20. Forest Products Laboratory. (1999). *Wood handbook: Wood as an engineering material* (Gen. Tech. Rep. FPL-GTR-113). U.S. Department of Agriculture, Forest Service. https://doi.org/10.2737/FPL-GTR-113

21. Franke, S., & Quenneville, P. (2013). Compression behavior and material parameters of radiata pine at different orientations to the grain. *Journal of Materials in Civil Engineering, 25*(10), 1514–1523. https://doi.org/10.1061/(ASCE)MT.1943-5533.0000699

22. Freitas, G. B., Rabelo, E. M., & Pessoa, E. G. (2023). Projeto modular com reaproveitamento de container marítimo. *Brazilian Journal of Development, 9*(10), 28303–28339. https://doi.org/10.34117/bjdv9n10-057

23. Garcia, A. G. (2025). The impact of sustainable practices on employee well-being and organizational success. *Brazilian Journal of Development, 11*(3), e78599. https://doi.org/10.34117/bjdv11n3-054

24. Gotardi Pessoa, E. (2022a). Análise comparativa entre resultados teóricos da deflexão de uma laje plana com carga distribuída pelo método de equação diferencial de Lagrange por série de Fourier dupla e modelagem numérica pelo software SAP2000. *Revistaft, 26*(111), 43. https://doi.org/10.5281/zenodo.10019943

25. Gotardi Pessoa, E. (2022b). Análise de custo de pavimentos permeáveis em bloco de concreto utilizando BIM (Building Information Modeling). *Revistaft, 26*(111), 86. https://doi.org/10.5281/zenodo.10022486

26. Gotardi Pessoa, E., Benittez, G. S. P., Oliveira, N. P., & Leite, V. B. F. (2022). Análise comparativa entre resultados experimentais e teóricos de uma estaca com carga horizontal aplicada no topo. *Revistaft, 27*(119), 67. https://doi.org/10.5281/zenodo.7626667

27. Gotardi Pessoa, E. (2024). Pavimentos permeáveis: Uma solução sustentável. *Revista Sistemática, 14*(3), 594–599. https://doi.org/10.56238/rcsv14n3-012

28. Gotardi Pessoa, E. (2025a). Analysis of the performance of helical piles under various load and geometry conditions. *ITEGAM-JETIA, 11*(53), 135–140. https://doi.org/10.5935/jetia.v11i53.1887

29. Gotardi Pessoa, E. (2025b). Optimizing helical pile foundations: A comprehensive study on displaced soil volume and group behavior. *Brazilian Journal of Development, 11*(4), e79278. https://doi.org/10.34117/bjdv11n4-047

30. Gotardi Pessoa, E. (2025c). Sustainable solutions for urban infrastructure: The environmental and economic benefits of using recycled construction and demolition waste in permeable pavements. *ITEGAM-JETIA, 11*(53), 131–134. https://doi.org/10.5935/jetia.v11i53.1886

31. Gotardi Pessoa, E. (2025d). Utilizing recycled construction and demolition waste in permeable pavements for sustainable urban infrastructure. *Brazilian Journal of Development, 11*(4), e79277. https://doi.org/10.34117/bjdv11n4-046

32. Gotardi Pessoa, E., Feitosa, L. M., Padua, V. P., & Pereira, A. G. (2023a). Estudo dos recalques primários em um aterro executado sobre a argila mole do Sarapuí. *Brazilian Journal of Development, 9*(10), 28352–28375. https://doi.org/10.34117/bjdv9n10-059

33. Gotardi Pessoa, E., Feitosa, L. M., Pereira, A. G., & Padua, V. P. (2023b). Efeitos de espécies de alna eficiência de coagulação, Al residual e propriedade dos flocos no tratamento de águas superficiais. *Brazilian Journal of Health Review, 6*(5), 24814–24826. https://doi.org/10.34119/bjhrv6n5-523

34. Grekin, M., & Surini, T. (2008). Shear strength and perpendicular-to-grain tensile strength of defect-free Scots pine wood from mature stands in Finland and Sweden. *Wood Science and Technology, 42*(1), 75–91. https://doi.org/10.1007/s00226-007-0151-8

35. Han, H., Yu, J., & Kim, W. (2018). Hair salon customers' perceptions of authenticity and its influence on satisfaction and loyalty. *Service Business, 12*(1), 1–23. https://doi.org/10.1007/s11628-017-0349-7

36. Hellmeister, J. C. (1973). *Sobre a determinação das características físicas da madeira* [Doctoral dissertation, São Paulo University].

37. Johnson, T. A., & Bankhead, T. (2014). Hair it is: Examining the experiences of Black women with natural hair. *Open Journal of Social Sciences, 2*(1), 86–100. https://doi.org/10.4236/jss.2014.21010

38. Karlsen, G. G., Bolshakov, V. V., Kagan, M. Y., Sventsitsky, G. V., Aleksandrovsky, K. V., Bochkaryov, I. V., & Folomin, A. I. (1967). *Wooden structures*. Mir Publishers.

39. Kollmann, F. F. P., & Côté, W. A. (1984). *Principles of wood science and technology: I. Solid wood*. Springer. https://doi.org/10.1007/978-3-642-87928-9

40. Liu, J. Y. (1984). New shear strength test for solid wood. *Wood and Fiber Science, 16*(4), 567–574.

41. Liu, J. Y. (2001). Strength criteria for orthotropic materials. In *Proceedings of the 8th Annual International Conference on Composite Engineering* (pp. 358–398). Spain.

42. Liu, J. Y., & Ross, R. J. (1998). Wood property variation with grain slope. In *Proceedings of the 12th Engineering Mechanics Conference* (pp. 17–20). La Jolla, CA, USA.

43. Logsdon, N. B., Finger, Z., & Jesus, J. M. H. (2014). Influência do ângulo entre o esforço aplicado e a direção das fibras da madeira sobre a resistência ao cisalhamento. *Ciência Florestal, 24*(4), 969–978. https://doi.org/10.1590/1980-509820142404016

44. Moreira, C. A. (2025). Digital monitoring of heavy equipment: Advancing cost optimization and operational efficiency. *Brazilian Journal of Development, 11*(2), e77294. https://doi.org/10.34117/bjdv11n2-011

45. NBR 7190-3. (2022). *Projeto de estruturas de madeira – Parte 3: Métodos de ensaio para corpos de prova isentos de defeitos para madeiras de florestas nativas*. ABNT.

46. Oh, S. C. (2011). Applying failure criteria to the strength evaluation of 3-ply laminated veneer lumber according to grain direction by uniaxial tension test. *Construction and Building Materials, 25*(4), 1480–1484. https://doi.org/10.1016/j.conbuildmat.2010.08.002

47. Oliveira, C. E. C. de. (2025). Gentrification, urban revitalization, and social equity: Challenges and solutions. *Brazilian Journal of Development, 11*(2), e77293. https://doi.org/10.34117/bjdv11n2-010

48. Padilha, V. H. L., Petrauski, A., dos Santos, A., Possa, D. C., Petrauski, S. M. F. C., & Savaris, G. (2023). Shear strength of pine wood bonded joints with different angles obtained using compression and torsional testing methods. *Revista Árvore, 47*, e4727. https://doi.org/10.1590/1806-908820230000027

49. Patel, A. K., Michaud, P., Petit, E., Baynast, H., & Grédiac, M. (2013). Development of a chitosan-based adhesive: Application to wood bonding. *Journal of Applied Polymer Science, 127*(6), 5014–5021. https://doi.org/10.1002/app.38097

50. Plaster, O. B., Oliveira, J. T. S., Gonçalves, F. G., & Motta, J. P. (2012). Comportamento de adesão da madeira de um híbrido clonal de *Eucalyptus urophylla* x *Eucalyptus grandis* proveniente de três condições de manejo. *Ciência Florestal, 22*(2), 323–330. https://doi.org/10.5902/198050985739

51. Raftery, G. M., Harte, A. M., & Rodd, P. D. (2009). Bonding of FRP materials to wood using thin epoxy gluelines. *International Journal of Adhesion & Adhesives, 29*(5), 580–588. https://doi.org/10.1016/j.ijadhadh.2009.01.004

52. Rodrigues, I. (2025). Operations management in multicultural environments: Challenges and solutions in transnational mergers and acquisitions. *Brazilian Journal of Development, 11*(5), e80138. https://doi.org/10.34117/bjdv11n5-103

53. Santos, H., & Pessoa, E. G. (2024). Impacts of digitalization on the efficiency and quality of public services: A comprehensive analysis. *Lumen et Virtus, 15*(40), 4409–4414. https://doi.org/10.56238/levv15n40-024

54. Serrano, E. (2004). A numerical study of the shear-strength-predicting capabilities of test specimens for wood-adhesive bonds. *International Journal of Adhesion & Adhesives, 24*(1), 23–35. https://doi.org/10.1016/S0143-7496(03)00096-4

55. Sherman, R., & Thompson, C. A. (2019). *Beauty and misogyny: Harmful cultural practices in the West*. Routledge.

56. Silva, J. F. (2024a). Enhancing cybersecurity: A comprehensive approach to addressing the growing threat of cybercrime. *Revista Sistemática, 14*(5), 1199–1203. https://doi.org/10.56238/rcsv14n5-009

57. Silva, J. F. (2024b). Sensory-focused footwear design: Merging art and well-being for individuals with autism. *International Seven Journal of Multidisciplinary, 1*(1). https://doi.org/10.56238/isevmjv1n1-016

58. Silva, J. F. (2025). Desafios e barreiras jurídicas para o acesso à inclusão de crianças autistas em ambientes educacionais e comerciais. *Brazilian Journal of Development, 11*(5), e79489. https://doi.org/10.34117/bjdv11n5-011

59. Stadlmann, A., Mautner, A., Pramreiter, M., Bismarck, A., & Müller, U. (2021). Interfacial adhesion and mechanical properties of wood-polymer hybrid composites prepared by injection molding. *Polymers, 13*(17), 2849. https://doi.org/10.3390/polym13172849

60. Szücs, C. A. (1992). Estudo do comportamento da madeira a esforços inclinados. In *4º Encontro Brasileiro em Madeiras e em Estruturas de Madeira* (Vol. 2, pp. 53–60). São Carlos, SP, Brazil.

61. Tannert, T., Vallée, T., & Hehl, S. (2012). Experimental and numerical investigations on adhesively bonded timber joints. *Wood Science and Technology, 46*(1–3), 579–590. https://doi.org/10.1007/s00226-011-0423-1

62. Testoni, F. O. (2025). Niche accounting firms and the Brazilian immigrant community in the U.S.: A study of cultural specialization and inclusive growth. *Brazilian Journal of Development, 11*(5), e79627. https://doi.org/10.34117/bjdv11n5-034

63. Thomas, L. M. (2020). Textured hair and the politics of representation in contemporary beauty culture. *Journal of Black Studies, 51*(7), 635–652. https://doi.org/10.1177/0021934720930933

64. Turatti, R. C. (2025). Application of artificial intelligence in forecasting consumer behavior and trends in e-commerce. *Brazilian Journal of Development, 11*(3), e78442. https://doi.org/10.34117/bjdv11n3-039

65. Vallée, T., Tannert, T., & Hehl, S. (2011). Experimental and numerical investigations on full-scale adhesively bonded timber trusses. *Materials and Structures, 44*(10), 1745–1758. https://doi.org/10.1617/s11527-011-9735-8

66. Venturini, R. E. (2025). Technological innovations in agriculture: The application of blockchain and artificial intelligence for grain traceability and protection. *Brazilian Journal of Development, 11*(3), e78100. https://doi.org/10.34117/bjdv11n3-007

67. Wang, T., Wang, Y., Debertolis, M., Crocetti, R., Wålinder, M., & Blomqvist, L. (2024). Bonding strength between spruce glulam and birch plywood at different load-to-plywood face grain angles. *European Journal of Wood and Wood Products*. https://doi.org/10.1007/s00107-024-02097-9

68. Wangaard, F. F. (1968). *The mechanical properties of wood* (1st ed.). Wiley.

69. Woodward, C. (1986). *The elastic and strength properties of Douglas fir in the radial-longitudinal plane* [Doctoral dissertation, New Mexico State University].

70. Woodward, C., & Minor, J. (1988). Failure theories for Douglas-fir in tension. *Journal of Structural Engineering, 114*(12), 2808–2813. https://doi.org/10.1061/(ASCE)0733-9445(1988)114:12(2808)

71. Xie, Y., Hill, C. A. S., Xiao, Z., Militz, H., & Mai, C. (2010). Silane coupling agents used for natural fiber/polymer composites: A review. *Composites Part A: Applied Science and Manufacturing, 41*(7), 806–819. https://doi.org/10.1016/j.compositesa.2010.03.005